Available online at www.sciencedirect.com
ScienceDirect
Mendeleev Commun., 2009, **19**, 187–189
Mendeleev Communications

Synthesis, chemical modification and electrochemical behaviour of layered sodium manganese dioxide

Victor V. De,[a] Ekaterina A. Pomerantseva,[a] Tatiana L. Kulova,[b] Anastasia V. Grigorieva,[a] Alexander M. Skundin,[b] Eugene A. Goodilin*[a,c] and Yuri D. Tretyakov[a,c]

[a] *Department of Materials Science, M. V. Lomonosov Moscow State University, 119991 Moscow, Russian Federation. Fax: +7 495 939 0998; e-mail: pomeran@inorg.chem.msu.ru*
[b] *A. N. Frumkin Institute of Physical Chemistry and Electrochemistry, Russian Academy of Sciences, 119991 Moscow, Russian Federation*
[c] *Department of Chemistry, M. V. Lomonosov Moscow State University, 119991 Moscow, Russian Federation*

DOI: 10.1016/j.mencom.2009.07.004

$Na_xMnO_2 \cdot nH_2O$ birnessite was used to yield one-dimensional nanostructures of manganese dioxide and effect of its chemical composition on electrochemical performance in lithium cells was studied.

Sodium manganese oxide with the birnessite structure is often used as a starting material in topotactic reactions with metal ions and organic molecules to hydrothermally prepare tunnel and sandwiched manganites.[1–3] Recently, it was demonstrated that δ-MnO_2 nanotubes can be synthesized through a controlled hydrothermal intercalation process by employing Na-birnessite as a precursor.[4] While manganese dioxide nanotubes are suggested as promising cathode material in lithium ion batteries, the reports on their synthesis are scarce and poorly reproducible. At the same time, Na-birnessite with a layered structure composed of edge-sharing MnO_6 octahedra forming the manganese oxide layers and sodium ions sited between the layers, can be used itself as a matrix for lithium intercalation. The birnessite-type manganese oxides can be prepared by redox precipitation processes,[5–7] sol–gel technique,[8,9] solid-state reaction,[4,10] and hydrothermal treatment.[11,12] The composition and electrochemical performance of birnessite-type manganese oxides is sensitive to formation reaction conditions.[13,14] In the solution processes, different amounts of water molecules can enter between the Mn–O layers together with sodium ions, forming materials with $Na_xMnO_2 \cdot nH_2O$ composition.[6,7] Na-birnessite was not extensively studied as a matrix for lithium intercalation, even though it is often used as a precursor for synthesis of different structures proposed as active cathode materials in lithium cells, like manganese oxides with tunnel crystal structures,[2,3] hybrid organic-inorganic materials[15] and manganese oxide nanotubes.[4] The reason is that Na-birnessite endures structural collapse resulting in rapid capacity fading.[16,17] The enhancement of the cycle performance of K-birnessite was achieved by Co doping.[18] Protonation in acidic media was demonstrated to be another way to improve the capacity retention during cycling, as it was shown for manganese oxides with tunnel crystal structures. Thus, for tunnel $Ba_6Mn_{24}O_{48}$ manganite, it was shown that initial acid treatment results in significant augmentation of lithium capacity and improvement of capacity retention during electrochemical cycling.[19,20] In this work, we have synthesized Na-birnessite using either solution or solid-state chemical routes and studied the electrochemical behaviour of its original and protonated forms in lithium cells.†

Figure 1 shows the XRD patterns of Na-birnessite obtained using either solid-state (sample 1) or solution (sample 2) method, as well as protonated $NaMnO_2$ (sample 3). For samples 1 and 2, the patterns correspond to the layered $NaMnO_2$ with a basal spacing of ~0.71 nm, which is consistent with literature data.[14]

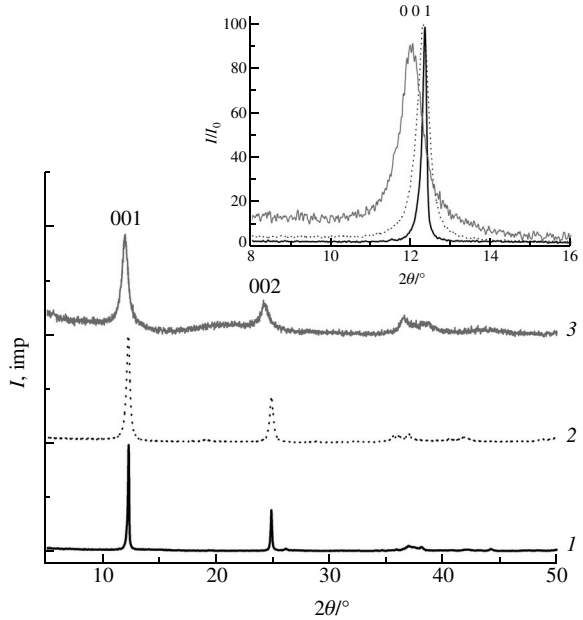

Figure 1 X-ray diffraction patterns of (*1*) Na-birnessite prepared *via* a solid-state route, (*2*) Na-birnessite prepared *via* a solution route and (*3*) H-form of Na-birnessite after an acid treatment of the sample (*2*). The inset shows an enlarged region of [001] reflection.

The spacing slightly expanded to ~0.73 nm after an acid treatment, which could be due to the protons incorporation into the interlayer space of Na-birnessite structure.[14,22] The Na:Mn ratios determined using EDX analysis are summarized in Table 1. Interestingly, the H-form of Na-birnessite is obtained very quickly and only 10–15 min of 1 M HNO_3 treatment is enough to extract almost all sodium ions from its structure, whereas for instance to prepare the H-form of $Ba_6Mn_{24}O_{48}$ tunnel manganite it takes five to eight days and concentrated nitric acid is needed.[22] In some

Table 1 Compositions of layered Na_xMnO_2.[a]

Sample number	Preparation method	Composition
1	Solid-state annealing	$Na_{0.974}MnO_2$
2	Precipitation from solution	$Na_{0.179}MnO_2$
3	Acid treatment of sample 2	$Na_{0.004}MnO_2$

[a]Compositions were determined from the EDX spectra collected from about ten randomly selected grains by assuming no oxygen deficiency.

papers, the authors report the amount of protons in manganites on the basis of charge compensation in the host MnO_2 structure or from the weight loss in the thermogravimetric curves.[14] However, according to our experience with the H-forms of manganese oxides, we find those estimations to be poorly effective, since protons can be incorporated into the manganites structure in different ways (as acidic protons, hydroxyl groups and water molecules), as well as adsorbed on the surface of the manganite particles in the large amount forming so-called water shell.[23] The diversity of proton forms makes it difficult to correctly determine the amount of protons in manganese oxides.

The presence of interlayer H_2O is usually determined from IR spectra of manganese oxides. For samples 2 and 3, Figure 2 indicates two prominent absorption bands at 3350 and 1620 cm^{-1} assigned to O–H stretching and H–O–H bending vibration of water molecule, respectively. In the IR spectrum of Na-birnessite prepared using solid-state annealing, those bands are less pronounced but still present. They can arise from H_2O molecules absorbed on the surface of the sample,[23] or from KBr rapidly absorbing water from air during samples preparation.

Figure 3 illustrates the electrochemical lithium cycling behaviour of the layered compounds synthesized in this work.

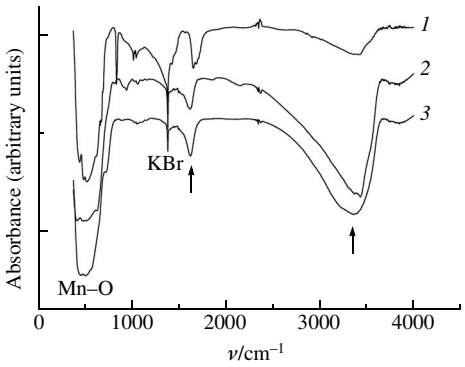

Figure 2 IR spectra of (*1*) Na-birnessite prepared *via* a solid-state route, (*2*) Na-birnessite prepared *via* a solution route and (*3*) H-form of Na-birnessite after an acid treatment of the sample (*2*).

The charge–discharge curves [Figure 3(*a*)] of the birnessite products demonstrate S-shape with a plateau at around 3 V typical of the manganese oxides with layered structure.[18,24–28] The layered Na-birnessite discharges in one step (one-electron reaction), and also the charging profile shows a one-step reaction. The shapes of the charge–discharge curves hardly depend on the Na:Mn ratio suggesting that the Li intercalation into birnessite was not remarkably affected by changes in the compostion. On the other hand, when we compare the maximum discharge capacities, the capacity of sample 1 is about 160 mAh g^{-1} whereas higher capacity of sample 2 (~180 mAh g^{-1}) and lower capacity of sample 3 (~145 mAh g^{-1}) were obtained. During the successive cycles, the capacity retention depends on the method of birnessite preparation and its composition. For samples 1 and 2, the maximum discharge capacities were reached at the second cycle and then the capacities gradually decreased during the following cycles. After 10 cycles, the discharge capacity of sample 1 decreased to ~115 mAh g^{-1} and the discharge capacity of sample 2 decreased to ~150 mAh g^{-1}; thus, their capacity retention ratios were about 72 and 83%, respectively. The acid treatment improved the capacity retention even though the value of the maximum discharge capacity for the acid treated

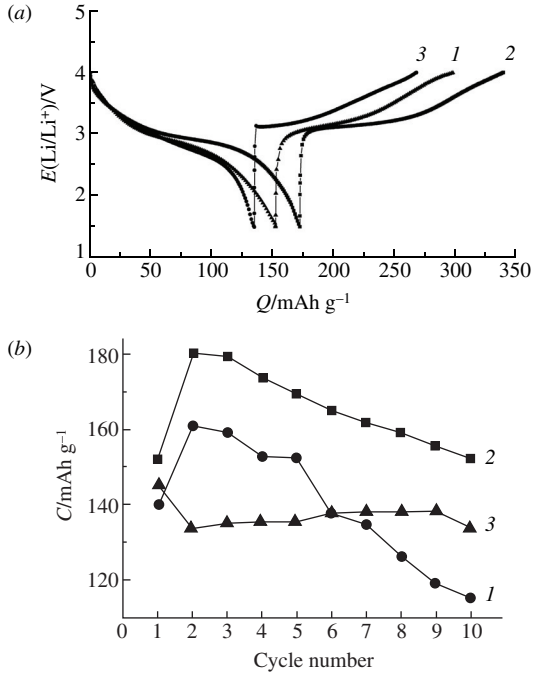

Figure 3 Cycling data at room temperature for lithium cells containing (*1*) Na-birnessite prepared *via* a solid-state annealing, (*2*) Na-birnessite prepared *via* a solution route and (*3*) H-form of Na-birnessite after an acid treatment of the sample (*2*): (*a*) charge–discharge curves for the fifth cycle; (*b*) discharge capacity *vs.* cycle number for the first ten cycles.

† $NaMnO_2$ ceramics was obtained using a conventional solid-state method[10] starting from high-grade Na_2CO_3 and Mn_2O_3 reagents mixed in a stoichiometric ratio, pressed into pellets and annealed at 850 °C in N_2 flow for 48 h. Alternatively, Na-birnessite was synthesized by a redox reaction between Mn^{VII} and Mn^{II} in water solution at room temperature as reported elsewhere.[21] $MnCl_2$ solution was added dropwise to the mixed solution of $KMnO_4$ and NaOH under vigorous stirring resulting in the formation of black precipitate (Na-birnessite). The precipitate was separated from the solution after aging for a day, washed thoroughly with distilled water until neutral pH and dried at 70 °C for ~12 h in air.

The protonated form (H-form) of Na-birnessite was prepared by treating the original material with a 0.1 M HNO_3 solution at room temperature for 15 min. After that, the powdered material was washed with distilled water until neutral pH and dried at 70 °C for ~12 h in air.

To obtain one-dimentional nanostructures of manganese dioxide, 0.5 g of Na-birnessite powder was dispersed in 35 ml of distilled water; then, the mixture was transferred into an autoclave and kept under hydrothermal conditions at 140 °C for about 96 h. The as-obtained brownish precipitate was washed with 1 M HNO_3 solution to remove sodium ions until pH 1. Thus obtained product was washed with distilled water until neutral pH and dried at 80 °C in air.

X-ray powder diffraction (XRD) data were taken with $CuK\alpha_1$ radiation at room temperature on a Bragg–Brentano-type powder diffractometer Rigaku D/Max-2500 with a rotating anode (Japan). The XRD data were measured in a 2θ range from 10° to 80° with a step interval of 0.02°.

Chemical composition of the samples (Na/Mn ratio) was determined by EDX analysis using a Leo Supra 50VP scanning electron microscope equipped with an INCA Energy+ EDX/WDX analyzer (Oxford). Transmission electron microscopy was used to obtain data for deciding on microstructural features of one-dimensional nanostructured systems (LEO 912 AB Omega with LaB_6 cathode).

The IR spectra of the samples were recorded on a Perkin Elmer FTIR spectrometer in the range of 350–7800 cm^{-1} using spectral pure KBr as a matrix. The samples (1 mg) were mixed with dry KBr (150 mg), annealed at 350 °C overnight before spectra acquisition and pressed into disks 0.1–0.2 mm thick.

Electrochemical insertion and extraction reactions were carried out using three-electrode lithium cells. The working electrode consisted of 80 wt% active material, 10 wt% acetylene black, and 10 wt% polyvinylidene fluoride dissolved in *N*-methylpyrrolidone. The mixture was pressed onto stainless steel grids and dried at 120 °C for 8 h in a vacuum and then moved to a glove box filled with Ar gas. The counter and reference electrodes were Li foils, and the separator was a microporous polypropylene sheet. The electrolyte was a 1 M solution of $LiClO_4$ in a mixture of propylene carbonate (PC) and dimethoxyethane (DME) (7:3, by volume). The cells were fabricated in an argon-filled glove box. Galvanostatic charge-discharge cycles were performed with the current density of 10 mA g^{-1} of active material using a multichannel potentiostat/galvanostat.

Na-birnessite was the lowest of all three samples. The discharge capacity for sample 3 decreased from 145 to 135 mAh g^{-1}; thus, the capacity retention ratio was about 93%. Note that starting from the second charge-discharge cycle, the discharge capacity of sample 3 is stable and its value is around 133–138 mAh g^{-1}.

The capacity values observed for sample 2 are higher than those for sample 1 [Figure 3(*b*)], which can be due to the steric and electrostatic factors caused by larger amount of sodium ions located in the interlayer space of the Na-birnessite obtained *via* solid-state route compared to the Na-birnessite prepared by precipitation from the solution (Table 1). In the crystal structure of sample 3, almost all sodium ions are replaced by protons (Table 1). This results in relatively low capacity values at the beginning of lithium cycling, but better capacity retention during longer cycling [Figure 3(*b*)]. According to literature[22,23] protons are fixed in the manganites structures due to the formation of Mn–O–H bonds and thus serve as structure stabilizing species, which is beneficial for electrochemical performance.

Use of nanostructured materials for energy storage recently demonstrated a series of phenomena ranging from high-rate performance to the development of new electrochemical processes including conversion reactions that can significantly increase the capacity of the system. The control of nanoparticle shapes can offer advantages of their use as active cathode materials in lithium cells.[29] For example, it was shown that the rate capability of Li intercalation in TiO_2 nanowires/nanotubes is better than the same phase prepared as isometric nanoparticles of a similar size.[29]

To synthesize MnO_2 nanotubes, we followed the procedure described elsewhere.[4] Figure 4(*a*) shows a typical morphology of one-dimensional particles obtained after the hydrothermal treatment of Na-birnessite obtained by solid-state reaction. According to the X-ray diffraction data [Figure 4(*b*)] the product of hydrothermal treatment has layered birnessite structure with the interlayer distance of ~0.71 nm. However, the overall product consisted of about half and half mixture of one-dimensional and globular particles, unlike data[4] where 100% MnO_2 nanotubes yield was reported. Also, according to TEM data it is hard to say if the obtained particles are nanotubes or nanorods [Figure 4(*c*)]. Cycling data for lithium cells containing the product of hydrothermal treatment are shown in Figure 4(*d*). The initial capacity value is about 212 mAh g^{-1}; however, it drops rapidly down to ~150 mAh g^{-1}. Thus, the search for optimal hydrothermal conditions is required to obtain pure MnO_2 nanotubes and study their electrochemical behaviour in lithium intercalation/deintercalation processes in detail. Further work in this direction is currently in progress.

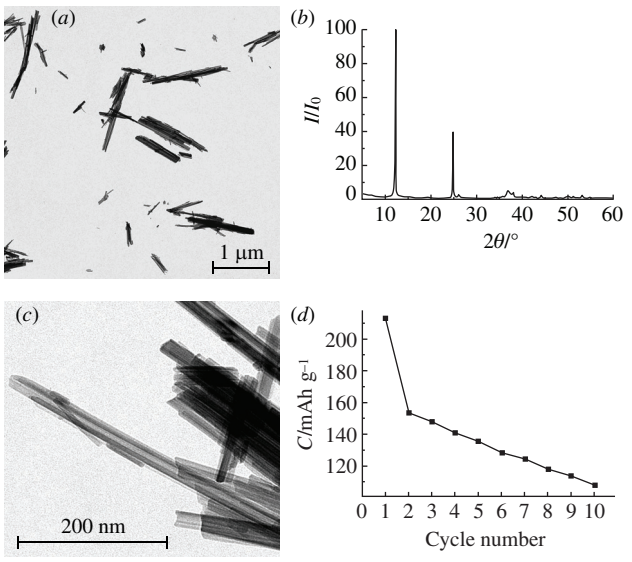

Figure 4 TEM images of MnO_2 one-dimensional structures and cycling data at room temperature for lithium cells containing the product obtained after hydrothermal treatment: (*a*) low magnification TEM image; (*b*) X-ray diffraction pattern of the product obtained after hydrothermal treatment; (*c*) high magnification TEM image and (*d*) discharge capacity *vs.* cycle number for the first ten cycles.

In conclusion, we have studied lithium intercalation/deintercalation behaviour in layered Na-birnessite with different Na:Mn ratio obtained using different synthetic approaches. We found that at the beginning of lithium cycling the H-form of Na-birnessite exhibits the lowest capacity compared to the original materials prepared *via* solid-state or solution methods. However, the capacity retention of the protonated form of Na-birnessite is ~93% after ten charge–discharge cycles which is dramatically better than that for the original materials.

We are grateful to I. V. Kolesnik, T. V. Philippova, D. M. Itkis and S. S. Abramchuk for their help in sample analysis. This work was supported by the Russian Foundation for Basic Research (grant no. 07-03-00749a) and FCNTP.

References

1 Q. Feng, H. Kanoh, Y. Miyai and K. Ooi, *Chem. Mater.*, 1995, **7**, 1722.
2 Q. Feng, K. Yanagisawa and N. Yamasaki, *J. Porous Mater.*, 1998, **5**, 153.
3 Q. Feng, C. Honbu, K. Yanagisawa and N. Yamasaki, *Chem. Mater.*, 1999, **9**, 2444.
4 X. Wang and Y. Li, *Chem. Lett.*, 2004, **33**, 48.
5 P. Strobel and C. Mouget, *Mater. Res. Bull.*, 1993, **28**, 93.
6 J. Luo and S. L. Suib, *J. Phys. Chem. B*, 1997, **101**, 10403.
7 Y. Ma, J. Luo and S. L. Suib, *Chem. Mater.*, 1999, **11**, 1972.
8 P. L. Golf, N. Baffier, S. Bach and J. P. Pereira-Ramos, *J. Mater. Chem.*, 1994, **4**, 133.
9 S. Ching, D. J. Petrovay, M. L. Jorgensen and S. L. Suib, *Inorg. Chem.*, 1997, **36**, 883.
10 J.-P. Parant, R. Olazcuaga, M. Devalette, C. Fouassier and P. Hagenmuller, *J. Solid State Chem.*, 1971, **3**, 1.
11 J. Morales, J. J. Navas and J. L. Tirado, *Solid State Ionics*, 1990, **44**, 125.
12 S. Hirano, R. Narita and S. Naka, *Mater. Res. Bull.*, 1984, **19**, 1229.
13 Y. J. Park and M. M. Doeff, *J. Power Sources*, 2007, **165**, 573.
14 Y. Omomo, T. Sasaki and M. Watanabe, *Solid State Ionics*, 2002, **151**, 243.
15 X. Zhang, L. Ji, S. Zhang and W. Yang, *J. Power Sources*, 2007, **173**, 1017.
16 A. Ogata, S. Komaba, R. Baddour-Hadjean, J.-P. Pereira-Ramos and N. Kumagai, *Electrochim. Acta*, 2008, **53**, 3084.
17 M. J. Duncan, F. Leroux, J. M. Corbett and L. F. Nazar, *J. Electrochem. Soc.*, 1998, **145**, 3746.
18 M. Tsuda, H. Arai and Y. Sakurai, *J. Power Sources*, 2002, **110**, 52.
19 E. A. Pomerantseva, Ya. Yu. Filippov, T. L. Kulova, A. M. Skundin, A. G. Veresov, E. A. Gudilin and Yu. D. Tret'yakov, *Dokl. Akad. Nauk SSSR*, 2007, **414**, 487 [*Dokl. Chem.* (*Engl. Transl.*), 2007, **414**, 140].
20 E. A. Pomerantseva, T. L. Kulova, Ya. Yu. Philippov, A. M. Skundin, E. A. Goodilin and Yu. D. Tretyakov, *Solid State Ionics*, submitted.
21 G.-G. Xia, W. Tong, E. N. Tolentino, N.-G. Duan, S. L. Brock, J.-Y. Wang and S. L. Suib, *Chem. Mater.*, 2001, **13**, 1585.
22 M. G. Kozlova, E. A. Gudilin, A. G. Veresov, E. A. Pomerantseva, L. S. Leonova, Yu. A. Dobrovol'skii and Yu. D. Tret'yakov, *Dokl. Akad. Nauk SSSR*, 2006, **411**, 66 [*Dokl. Chem.* (*Engl. Transl.*), 2006, **411**, 197].
23 Y. Chabre and J. Pannetier, *Prog. Solid State Chem.*, 1995, **23**, 1.
24 S. H. Kim, S. J. Kim and A. M. Oh, *Chem. Mater.*, 1999, **11**, 557.
25 S. H. Kim, W. M. Im, J. K. Hong and A. M. Oh, *J. Electrochem. Soc.*, 2000, **147**, 413.
26 C. Julien, M. Massot, R. Baddour-Hadejean, S. Franger, S. Bach and J.-P. Pereira-Ramos, *Solid State Ionics*, 2003, **159**, 345.
27 S. Franger, S. Bach, J. Rarcy, J.-P. Pereira-Ramos and N. Baffier, *J. Power Sources*, 2002, **109**, 262.
28 R. Chen, P. Zavalij and M. S. Whittingham, *Chem. Mater.*, 1996, **8**, 1275.
29 A. S. Arico, P. Bruce, B. Scrosati, J.-M. Tarascon and W. Van Schalkwijk, *Nat. Mater.*, 2005, **4**, 366.

Received: 19th February 2009; Com. 09/3286